ELSEVIER Journal of Hazardous Materials 46 (1996) 215–223

JOURNAL OF HAZARDOUS MATERIALS

Dense gas simulation flows over rough surfaces

Wayne D. Peters, Steven R. Cogswell, James E.S. Venart*

Fire Science Centre, University of New Brunswick, Fredericton, New Brunswick, Canada

Received 29 April 1994; accepted 27 January 1995

Abstract

Mixing within a gravity current head, passing over a rough surface, is assessed using a two-dimensional quantitative full-field flow visualization technique. The method combines salt-water modelling, laser-induced dye fluorescence and video image enhancement. The mixing mechanisms that occur internal to the head structure are shown to play a major role in the overall dilution process and to be significantly affected by surface roughness. The effect of surface roughness is consequential for the accurate prediction of heavier-than-air gas dispersions, for instance. Flows with Reynolds numbers of 500, 1000 and 1500 and density differences of 0.5, 1.0 and 1.5% are considered. Results are presented for flows over two surface types – smooth and rough with a relative roughness element height of 0.35 and frontal obstruction of 50% based on roughness element diameter.

Keywords: Dense gas dispersions; Roughness; LIF

1. Introduction

Gravity currents are buoyancy-driven flows that produce motions normal to the gravitational field. The horizontal flow structure consists of a head at the leading edge of the flowing layer, with a slightly elevated nose, under which less dense ambient fluid can be ingested. As the fluid advances, mixed fluid settles into the area behind the head and above the feeding current layer, forming a layer of intermediate density mixed fluid between the current and ambient fluids.

In order, to evaluate current dilution levels, it is necessary to understand the interchange processes involved. Two mixing mechanisms, and their sites, have been defined by the work to date at UNB and elsewhere. Firstly, Kelvin–Helmholtz instabilities, initiated by the velocity shear at the intruding head/ambient fluid interface, lead to mixing in the head region. This results in billows and waves that flow

* Corresponding author.

0304-3894/96/$15.00 © 1996 Elsevier Science B.V. All rights reserved
SSDI 0304-3894(95)00073-9

up over the head and settle in the mixed layer behind. Secondly, mixing internal to the head region arises as a layer of lighter ambient fluid is over-run by the advancing head. The velocity shear between this over-run fluid and the current head causes further Kelvin–Helmholtz instabilities at this level. However, as this fluid is buoyantly unstable, Taylor instabilities further contribute to, and perhaps even dominate, the internal mixing.

2. Review of past work

Salt-water modelling has been shown to be very useful in the study of buoyancy driven flows. Peters et al. [1], Zukoski and Kubota [2] and Chobotov et al. [3] have all used the technique to examine flows in horizontal channels or corridors. Steckler et al. [4] also employed the method to simulate fire induced buoyant flows in multi-compartment enclosures.

Simpson [5–7] and Simpson and Britter [8] have studied gravity currents using this technique. In a comprehensive examination, they concluded that the shear between the gravity current head and ambient fluid was the main mixing process at the front [8]. They stated that the flux of light fluid flowing under the head (estimated to be of the order of 0.01 of that involved in mixing at the top of the head) may be neglected as a contribution to overall mixing.

The work of Simpson [5–7] and Simpson and Britter [8] dealt primarily with smooth surface flows. Aside from the work of Simpson [7], in which roughness was considered in the form of a porous fence greater in height than the head, no other references examining salt-water flows over rough surfaces have been found.

Using lock exchange experiments, Winant and Bratkovich [9], however, observed large fluctuations in density in the head region. They concluded that lighter fluid was entrained at the very leading edge and the density variations seemed to be more a result of gravitational instability between discrete parcels of unmixed fluid rather than any active turbulent fluctuations.

Surface roughness effects on the dispersion of heavier-than-air gas clouds were considered by Petersen and Ratcliff [10] and Petersen [11] for the American Petroleum Institute using a wind tunnel facility. Primarily concerned with roughness scales that are large compared with the size of the cloud, they stated that current numerical models for gas dispersions have only been tested against field data bases collected in flat homogeneous terrain.

They determined that cloud concentrations in a dispersion over surface roughness, typical of an urban area, were reduced by as much as 25 times over those found for a spread over a grassy plain. It is therefore important to consider the influence of roughness. Roberts et al. [12] further considered the data of Petersen and Ratcliff [10] in an attempt to validate typical dispersion models. They also concluded that current integral models of dense gas dispersion are limited to predictions over grasslands or open sea. This further emphasizes the need for basic work on releases over rough terrain.

3. Scaling laws

The gravity current Reynolds number can be defined in terms of (1) the feeding current layer depth, H, and the head frontal velocity, u_2, [8] or (2) the feeding current layer depth, H, and velocity, U [2]. Fundamentally, the second of these definitions appears to be more appropriate as it is based on parameters that directly describe the source condition of both experiment and simulated events (dense gas dispersion or cold weather fronts). Based on continuity, the product of these variables in the second instance is the source injection rate per unit channel width, Q, and can be used to define the Reynolds number. A Froude number, based on these same parameters, can also be defined.

Reynolds numbers in the range 250–5000 with density variations, $\Delta\rho/\rho_A$, of 0.004–0.15 have all been utilized in the past [2, 8]. The Froude numbers and ratios of mixed layer to current layer depth, $(h_2 - H)/H$, were, thus, varied from 0.75 to 1.30 and from 0.50 to 3.0, respectively. These values were obtained over a range of fractional depth of the gravity current to the overall fluid height, H/h_1, of 0.05–0.30 for smooth channel flow only [8]. The values of these parameters in this work are similar.

4. Experimental technique

The flows are created in an open plexiglass channel, 230 cm long and 20 cm wide with a maximum depth of 30 cm using a technique described in detail in Ref. [1]. Saline fluid enters through an upstream entry section on the channel bottom and, after spilling over an inlet edge, flows down the channel length to form the intruding current.

The full channel length for these tests is arranged to illustrate flow behaviour before, during and after the effects of a roughness array. In the cases reported here, the roughness section is formed by cementing aluminium cylinders onto a mylar sheet laid on the floor. This roughness section consists of a 70 cm long staggered array of cylinders, 12.5 mm diameter × 6.0 mm high at 25 mm spacing, positioned across the full channel width and follows an initial 75 cm smooth section. A final 85 cm long section allows the current to recover from the roughness array and re-establish before its impact at the vertical end wall of the tank.

Visualization of the flow is facilitated through laser-induced fluorescence (LIF). A vertical laser sheet is passed through the channel on its longitudinal mid-plane. The introduced saline gravity current contains fluorescein sodium in low concentration (0.02 mg/l). This dye fluoresces at 515 nm when excited by the 488 nm blue line of an argon ion laser.

Experiments are recorded in real-time (30 frames/s) S-VHS format using a solid state B/W CCD video camera (Panasonic WV BD-400) equipped with a low-light level image intensifier (Astrolight 9100). The flow illumination and video system is mounted on a stepper motor driven traversing carriage. The speed, acceleration/deceleration and direction of the carriage can be maintained and/or altered while the gravity current head is tracked. During steady-state tracking conditions, the

gravity current advance remains motionless relative to the traversing system, allowing a time-averaged quantitative analysis of the resulting videos.

Video images are processed using a PC-based image processing system consisting of a 486 based PC-AT compatible computer equipped with a MATROX MVP-AT/NP frame grabber board (512 × 512 resolution). Use of this system, along with custom and commercial software packages for image processing allows single snapshots and time-averaged segments to be grabbed and analysed from real-time video, and stored as image files for post-processing and analysis.

5. Test matrix and observations

Three series of tests were performed at density differences of 0.5%, 1.0% and 1.5% with Reynolds numbers of 500, 1000 and 1500 with the fixed roughness array described earlier. Each test consists of observations of the gravity current before, during and after interaction with the roughness array as it flows down the channel.

Table 1 summarizes the dimensionless normalized parameters of interest for a typical experiment for flow (a) prior to the roughness section, (b) over the roughness section, and (c) after the roughness section. The test reported is for a Reynolds number of 1000 and density difference of 1.0%. The feeding current layer depth, H, and velocity, U, for the pre-roughness case are used to normalize the data and yield the dimensionless variables of Table 1. A typical image with concentration contour map time-averaged over 30 frames at 30 frames/s is given in Fig. 1 for the same flow.

The parameters H, h_2, h_3 and L are scaled from the processed images. In the case of the internal mixing length, L, density contour maps were used to estimate the position at which the internal feeding current layer breaks down due to mixing internal to the head. This position is defined as the furthest penetration into the head region of the contiguous feeding current layer.

The mean feeding current layer velocity, U, is derived from the known injection rate per unit channel width, Q, and the observed feeding current layer depth, H, such that

Table 1
Roughness influence on the gravity current flow parameters with $Re = 1000$ and $\Delta\rho/\rho_A = 0.010$

Parameter	Pre-roughness	Roughness	Post-roughness
H^*	1.00	1.29	0.82
h_1^*	17.65	17.65	17.65
h_2^*	2.82	3.53	2.82
h_3^*	0.41	0.71	0.47
h_R^*	~0	0.35	~0
L^*	2.1	7.4	7.4
U^*	1.00	0.78	1.22
u_2^*	0.67	0.52	0.55
$(U^* - u_2^*)/U^*$	0.33	0.48	0.45

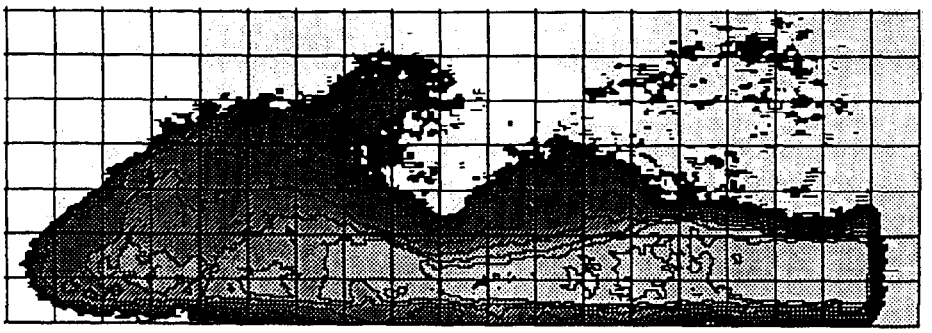

Fig. 1. Image of a gravity current advancing over the channel roughness section with its concentration contour map superimposed on it. $Re = 1000$. $\Delta\rho/\rho_A = 0.01$. The grid is marked in 1 cm increments.

$U = Q/H$. The mean observed current head frontal velocity, u_2, is taken as the video system tracking velocity when steady-state tracking conditions are achieved. From mass continuity, the velocity, U, must be greater than the velocity, u_2, to provide an influx of dense fluid to feed the mixing occurring in the head. The difference, $(U - u_2)$, represents the velocity at which the feeding current layer overtakes the head. The mixing at the head, therefore, can be expressed as the ratio, $(U - u_2)/U$, quantifying the overall fraction of total dense fluid influx that is mixed.

6. Discussion

The trends observed in the data of Table 1 are typical for a head advance down the channel and over the roughness section. The dynamics and structure of the head are observed to alter significantly as it passes from the smooth to rough surface.

A growth in the current head height, h_2, and the feeding current layer depth, H, is rapidly apparent as the head frontal velocity, u_2, and the feeding current layer velocity, U, decrease under the influence of a rougher surface. The increase in the normalized head height, h_2^*, indicates that this growth is more significant for the current head.

The internal mixing length, L^*, increases by a factor of 3.5 with increase in the roughness scale, h_R^*. As well, the overall mixing ratio, $(U^* - u_2^*)/U^*$, is seen to increase by approximately 45%. Internal mixing with roughness is, therefore, greater as evidenced by the increase in these parameters.

The increase in the normalized nose height over the roughness section allows, in this case, a greater amount of less dense ambient fluid to become ingested under the head. This trapped fluid then becomes available to enhance internal mixing.

It appears that the mixing in this region is caused by Taylor instabilities – packets of buoyantly unstable over-run fluid rising through the structure – and Kelvin–Helmholtz instabilities – evidenced by a periodic mixing disturbance near the boundary. The extent of this mixing, within the gravity current head, leads to an increased

horizontal density gradient and appears to be much greater than that which can be attributed to the lobe and cleft formation discussed by Simpson [6].

After passing from rough to smooth surfaces, the current head structure, defined by h_2^* and h_3^*, reverts back to its pre-roughness shape. The internal mixing length and the mixing ratio, however, indicate that the head structure is still significantly affected by the prior mixing. It appears that this influence persists downstream at least 60H.

The mixing within the structure of a gravity current can be characterized by the internal mixing length, L^*, and the overall mixing ratio, $(U^* - u_2^*)/U^*$. In this set of experiments, they appear to be more sensitive to changes in the Reynolds number than in the density difference. Figs. 2 and 3 show these parameters as a function of the Reynolds number.

Both figures indicate that the rough surface increases the internal current mixing by a factor of nearly 2 for both L^* and $(U^* - u_2^*)/U^*$ at low Reynolds numbers. The sensitivity of these parameters with $\Delta\rho/\rho_A$ is indicated in the figures by the variance bands for the different density test points at constant Reynolds number. It is observed that the influence of density difference is not as significant as that due to roughness or Reynolds number and that this dependence is negligible for the rough surface cases.

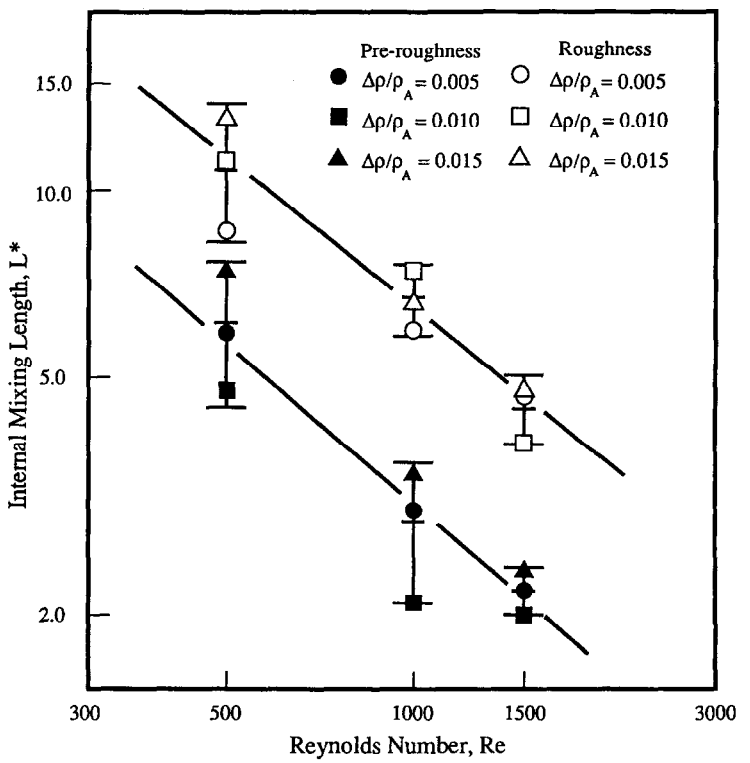

Fig. 2. Influence of Reynolds number, Re, and density difference, $\Delta\rho/\rho_A$, on the internal mixing length, L^*.

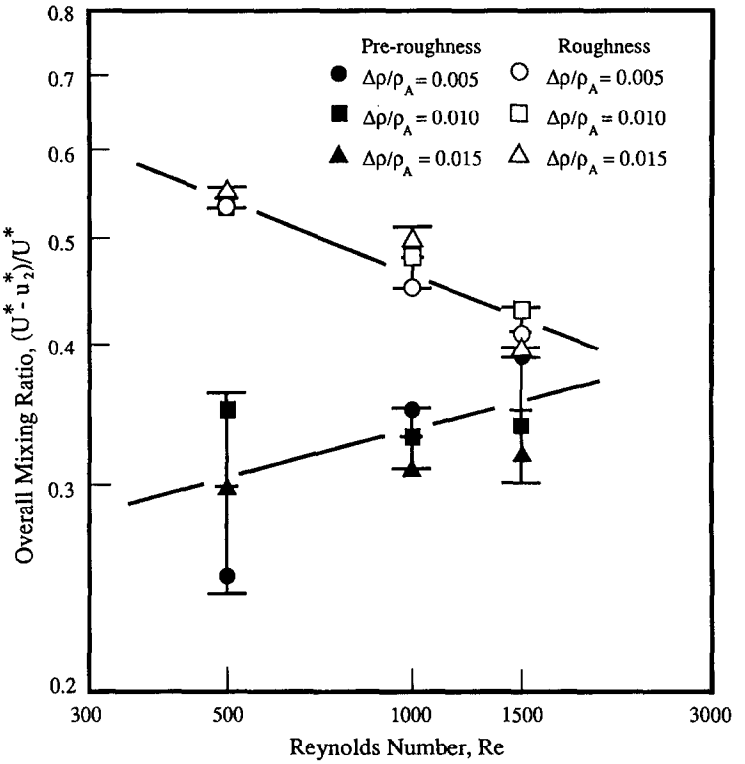

Fig. 3. Influence of Reynolds number, Re, and density difference, $\Delta\rho/\rho_A$, on the overall mixing ratio $(U^* - u_2^*)/U^*$.

Fig. 2 shows the dependence of the internal mixing length, L^*, with Reynolds number. The increased mixing length due to the roughness is clearly evident over the full Reynolds number range. As the Reynolds number increases, the current head height, h_2^*, and the feeding current layer depth, H^*, increase, thus decreasing the relative roughness scale, h_R^*, and the mixing as evidenced by decreasing L^*.

The same argument can be applied in Fig. 3 which considers the variation of the overall mixing ratio, $(U^* - u_2^*)/U^*$, with Reynolds number. Again, mixing seems to be insensitive to the density difference over the range tested. Roughness has a much greater effect. Again, the mixing over the rough surface is seen to decrease with increasing Reynolds number. In the limit, the rough surface mixing ratio should, however, approach that of the smooth surface as the relative roughness height decreases.

7. Conclusions

The influence of surface roughness on the advance of a gravity current was assessed for Reynolds numbers of 500, 1000 and 1500 with density differences of 0.5%, 1.0%

and 1.5%. In each case, the images and density contour maps indicate that the extent of the internal mixing length, L, and the overall mixing ratio, $(U^* - u_2^*)/U^*$, increase as the current passes over the roughness array. The increased roughness, also, raises the nose slightly during advance allowing more lighter fluid to be ingested into the region internal to the head to produce even greater mixing due to Taylor instabilities.

Figs. 2 and 3 support the conclusion that surface roughness greatly increases the amount of internal mixing over the range of Reynolds numbers tested. The extent of this effect is much more significant than that of the density difference over the small range tested. For this work, the density difference effect has not, as yet, been resolved.

The appearance of mixing disturbances and packets of unmixed over-run fluid in the internal region of the head (Kelvin–Helmholtz and Taylor instabilities) as evidenced in the images and density contour maps, confirms the observations and conclusions of Winant and Bratkovich [9]. This evidence strengthens our conclusion that substantial mixing occurs within the head region due to the ingestion of lighter over-run fluid. This factor should increase with roughness and be dependent on the roughness element scale and distribution.

8. Future work

It has been shown here that surface roughness greatly increases the mixing at the current/boundary interface. Flows over regular patterns of different roughness elements will be assessed. The influence of the scale and number density of the surface roughness elements will be studied to better understand current dilution over various types of surfaces. At present, very little data are available for these situations.

It is anticipated that lighter ambient fluid can become trapped in the space between roughness elements as the current head advances and over-runs it. The amount of this buoyantly unstable fluid should depend on the roughness element number density and size. This fluid is then available to promote increased vertical mixing and, thus, influence the current advance, provided the Reynolds number is small. This work should be important to dense gas dispersion models [13] and supplement wind tunnel simulations [10, 11].

Nomenclature

H	feeding current layer depth, cm
L	internal mixing length, cm
Q	injection rate per unit width, cm^2/s
U	feeding current layer velocity, cm/s
h_1	ambient fluid depth, cm
h_2	current head height, cm
h_3	nose height, cm
h_R	roughness element height, cm
u_2	current head frontal velocity, cm/s

Greek symbols

ρ_A	ambient fluid density, g/cm^3
ρ_B	current fluid density, g/cm^3
ν_B	current fluid viscosity, cm^2/s

Acknowledgements

Past and ongoing support from Emergency Preparedness Canada, the Natural Sciences and Engineering Research Council of Canada and the Society of Fire Protection Engineers has made it possible to continue this research.

References

[1] W.D. Peters, C.R. Dutcher and J.E.S. Venart, in: Proc. 3rd Symp. on Experimental and Numerical Flow Visualization, 1993 ASME Winter Annual Meeting, New Orleans, LA, 28 November–3 December 1993, ASME FED Vol. 172, p. 285.

[2] E.E. Zukoski and T. Kubota, Experimental study of environment and heat transfer in a room fire, Report No. NIST-GCR-88-554, Center for Fire Research, National Institute of Standards and Technology, Gaithersburg, MD, 1988.

[3] M.V. Chobotov, E.E. Zukoski and T. Kubota, Gravity currents with heat transfer effects, Report No. NBS-GRC-87-522, Centre for Fire Research, National Bureau of Standards, Gaithersburg, MD, 1986.

[4] K.D. Steckler, H.R. Baum and J.G. Quintiere, in: Proc. 21st Symp. (Int.) on Combustion, The Combustion Institute, 1986, p. 143.

[5] J.E. Simpson, J. Fluid Mech., 53(4) (1972) p. 759.

[6] J.E. Simpson, Acta Mech., 63 (1986) 245.

[7] J.E. Simpson, Gravity Currents: In the Environment and the Laboratory, Ellis Horwood Limited, West Sussex, UK, 1987.

[8] J.E. Simpson and R.E. Britter, J. Fluid Mech., 94(3) (1979) 477.

[9] C.D. Winant and A. Bratkovich, in: Proc. 6th Australasian Hydraulics and Fluid Mechanics Conf., Adelaide, Australia, 5–9 December 1977.

[10] R.L. Petersen and M.A. Ratcliff, Effect of homogeneous and heterogeneous surface roughness on heavier-than-air gas dispersion, API Publication No. 4491, Washington, DC, 1989.

[11] R.L Petersen, Surface roughness effects on heavier-than-air gas diffusion, API Publication No. 4459, Washington, DC, 1987.

[12] P.T. Roberts, J.S. Puttock and Blewitt, Gravity spreading and surface roughness effects in the dispersion of dense gas plumes, For presentation at the A.I.Ch.E. 1990 Health and Safety Symp., Session IIB: Modelling of Aerosol Clouds, Orlando, FL, 18–22 March, 1990.

[13] D.R. Blackmore, M.N. Herman and J.L. Woodward, J. Hazard. Mater., 6 (1982) 107.